Acta Acustica united with Acustica
Vol. 102 (2016) 930 – 937

DOI 10.3813/AAA.919007

A New Approach for Estimating Noise Emission of Automotive Vehicles

David Ibarra, Ricardo Ramírez-Mendoza, Edgar López
Tecnológico de Monterrey, Escuela de Ingeniería y Ciencias, Campus Mexico City, Calle del Puente 222, Ejidos de Huipulco, Tlalpan, 14380, Mexico D.F. david.ibarra@itesm.mx

Summary
Current systems for measuring traffic noise are based on an overall assessment, so that they are unable to discriminate between type of vehicle and noise propagation. In this work we propose a near-field noise measuring method that is able to measure the contribution of each vehicle to the road traffic noise, allowing the characterization and quantification of different types of vehicles. This paper also describes a combination of analytical and experimental investigations for a methodology to carry out noise analysis for automotive vehicles. The system is based on two on-board microphones, one for the engine noise and the other for the rolling noise. In order to relate these near-field (0–0.1 m from the source) measurements with the noise radiated from the vehicle to the far-field (at 7.5 m from the source), a complete procedure was developed for the extrapolation of the near-field noise to the far-field positions with a combination of analytical models. Corrections for the extrapolated levels were made taking into account atmospheric factors, the spherical spreading term and the absorbing conditions of the propagation on the surface. For the microphone situated close to the engine it was also necessary to estimate the acoustic properties of the engine hood. Both noise levels were extrapolated independently of the far-field position, for which a noise level was predicted in order to estimate the remote noise impact to the overall traffic noise.

PACS no. 43.28.Fp, 43.28.Gq

1. Introduction

The issue of road traffic noise needs a new and audacious approach that contributes to alleviate the noise annoyance, which is of both scientific and sociological interest. In this context, and taking into account that noise annoyance is highly correlated with the maximum noise levels [1] radiated by the most noisy vehicles, a methodology, based on the on-board measurement of the noise radiated by each vehicle to the near field, is proposed in this study to detect those vehicles. The main contribution of this paper is to propose a suitable way to categorize between vehicle type and noise propagation, which describes a combination of analytical and experimental manners to carry out noise analysis for automotive vehicles, this approach represents an integration of research results reported by Ibarra *et al.* [2, 3, 4, 5]. They are preliminary results and part of a methodology, which is presented here for noise emission of any passenger car. Such an on-board system should facilitate an historical record of the noise radiated by each vehicle. On one hand, it would provide a tool for a fairer administrative control of traffic noise, helping to detect the noisiest vehicles in periodical vehicle technical inspections. On the other hand, it would facilitate a more precise approach to traffic noise studies, in more realistic conditions, including effects such as the vehicle segment, engine type, vehicle age, and road maintenance.

Some considerations to explain the problem of road traffic noise include [6]:

- The operating conditions for the type approval tests are not sufficiently representative of actual driving mode.
- The increase in traffic volume, as well as the trend towards more powerful vehicles with wider wheels, which results in higher noise emissions, cancel out the benefits of reductions in emission limits.

2. Noise sources

A vehicle produces noise from various sources, such as the power unit (including the engine, air inlet and exhaust), the cooling fan, the transmission system (including the gearbox and rear axle), the rolling (including the aerodynamics and the tire/pavement components), the brakes and the load [7, 8]. In general, the noise related to the power unit and the transmission is referred to as engine noise, while noise related to the other sources is referred to as rolling noise.

In the case of light-weight vehicles, the engine noise dominates at low speeds and low gears (1st, 2nd gears), whereas the rolling noise dominates at high speeds and

Received 23 October 2015,
accepted 23 June 2016.

higher gears (3rd, 4th, 5th gears) [9]. However, in heavy vehicles the engine is the dominant source under all operating conditions, although the rolling noise can be noticeable also at high speeds.

Taking into account that in this work we are proposing a methodology to assess the noise radiated by a vehicle under all operating conditions, including urban (low speed) and suburban (high speed) running, both noise sources will have to be considered.

From the near to far fields, these noise sources must be combined logarithmically to provide the overall vehicle noise. The noise spectra radiated by light-weight vehicles at a distance of 7.5 m cover a substantial part of the audible range, and they usually have defined peaks at the low frequency side. For most vehicles, far-field noise spectra above 2–3 kHz decays linearly with frequency [7, 8]. Sandberg reported a multi-coincidence peak at around the 1000 Hz octave in the traffic noise spectra [10].

Affenzeller and Rust [11] studied the contribution of each of these sources to the overall noise emission of vehicles during the approval test established in the ISO 362 standard [12]. The relative contribution of the sources has varied over time. Before 1990, the main contributor to the overall pass-by noise was the engine, while at the time of writing it was the tire-pavement interaction. In section 3 we explain the characteristics of these sources of vehicle noise in the near-field.

3. Methods of measurement of vehicle noise emission

There are already four standardized methods for measuring the noise radiated by the vehicle to the near- (CPX) and far- (SPB/CPB/SPB-BB) fields:

- The Statistical Pass-By (SPB) method based on the ISO 11819-1 [13]: Measurement of the influence of road surfaces on traffic noise: Part 1.
- The Close Proximity (CPX) method based on the ISO/CD 11819-2 [14]: Measurement of the Influence of road surfaces on traffic noise: Part 2.
- The Statistical Pass-By (SPB-BB) method using backing board based on the ISO/PAS 11819-4 [15]: Method for measuring the influence of road surfaces on traffic noise: Part 4.
- A fourth widely used method, the Controlled Pass-By Method (CPB), which is basically a variant of the SPB method, where a small number of test vehicles are chosen to represent general types of vehicles required in the SPB method.

The SPB methods provide a tool to determine an index, which can be used to compare the noise emission impact of different road surfaces, by measuring a number of vehicle passes-by at the roadside [16].

The CPB method was conceived for evaluating the influence of various road surfaces on traffic noise, under conditions when tire/road noise dominates. The interpretation of the results applies to free-flowing traffic traveling on essentially level roads at constant speeds of 40 km/h or more, in which cases tire/road noise is assumed to dominate.

Figure 1. Position of the engine microphone close to the air intake system.

Measurements with the CPX method are faster and more practical than with the SPB method, but are more limited in the sense that they are relevant only in cases where tire/road noise dominates and engine noise may be disregarded.

The SPB method was devised for assessing the effect of the road surface on the traffic noise, measured at the front of dwellings (far-field), while the CPX method was designed to characterize the noise emission from roads (near-field); therefore, there is a relationship between the two methods. In principle, it may be possible to predict the SPB levels from the CPX measurements on an arbitrary road surface. The relationship between the CPX and SPB levels has been studied in depth by the European Commission (EC) projects SILVIA [17, 18, 19] and SILENCE [20].

The studies, however, have not been able to show reproducibility across the SPB/CPB-CPX relation from one site to another is, perhaps, that the effect of the different type of surfaces in each of the two positions was not taken into account. This was carried out, in the context of the EC Project SILVIA, by Anfosso-Lédée [19].

Cho and Mun [21] published a semi-empirical model for the determination of sound power levels emitted by vehicles to the near- and far-fields that has been successfully applied in prediction models of road traffic noise in South Korea [22]. Similarly to Anfosso-Lédée, Cho and Mun analyzed the propagation of noise between NCPX (Novel Close Proximity method) and SPB positions.

In the present study we decided to use two microphones to measure the contributions of the engine and tire/road interaction to the vehicle noise in the near-field. According to Stücklschwaiger [23], the microphone to pick up the engine noise was located close to the air intake manifold, as this makes the largest contribution to noise from this source, Figure 1. Also, the noise from the intake system can be categorized as primary source noise [24, 25]. This location also has the advantage of avoiding overheating of the microphone by the engine. To measure the rolling noise in real driving conditions (influence of wind-induced microphone noise), it was necessary to disregard

the positions for the microphone recommended by the CPX method. Instead, the microphone was located below the car chassis, close to the tire, Figure 2. This location is similar to that chosen by Cho and Mun [21] in their measurement set up, except that they mounted theirs on the wheel arch in order to take into account the horn effect [26] of the rolling noise amplification due to the existing geometry between tire and surface. This geometry amplifies the noise because of the reflections on the contact area, so that the generated radiation power is greater at the base. This phenomenon was verified experimentally by Iwao *et al.* [27] using a real tire. Other experimental measurements [28] show amplification due to the horn effect of 10 to 20 dB, with a maximum in the plane of the tire.

Figure 2. Position of the rolling microphone close to the rear wheel for the rolling noise measurement.

4. Experimental setup

This part of the study describes a sample scenario for the measurement of noise emitted by cars, and the next paragraphs explain some relevant issues to be considered. The methodology was able to characterize the noise emitted by an individual vehicle. We show in a general way the main aspects of this experimental setup on a complete urban circuit, as shown in Figure 3 and Figure 4.

On-board measuring devices have been previously used for driver identification purposes [29] and for measuring the quality of traffic flow [30].

Simultaneously, information about the driving performance can be picked up from the CAN BUS interface of the vehicle which includes an ODB2 module. This system is interfaced to the acquisition system through an ELM327 probe, allowing picking up information of three signals, namely, the engine speed, the engine load, and the position of the accelerator. Analysis of coincident acoustical/driving performance data in real driving conditions will allow setting the correlation, if any, between the noise emitted by individual vehicles and the driving style [3, 4, 5]. The drivers for the test were experienced drivers, able to drive any vehicle, and without physical disabilities.

Due to the risk of damage under the experimental conditions, and the position under the vehicle chassis, creating problems with dust, humidity, etc., it was decided to use electret microphones with good enough acoustical characteristics. Electret microphones maintain their own polarization, eliminating the potential for condensation in high-humidity environments and they are often less sensitive at high frequencies [31]. Technical specifications of the microphones used are summarized in Table I. The polar pattern of the microphones was omnidirectional and their frequency response was 20 to 20,000 Hz. Both the maximum sound pressure level (125 dB) and dynamic range (91 dB) were clearly sufficient for the measurement of engine and rolling noises in real driving conditions.

The signals recorded by the microphones were then analyzed with the PULSE LabShop system, which is a hardware/software data acquisition system. When the measurements were carried out the weather conditions were registered as temperature, relative humidity, atmospheric pressure, and wind speed.

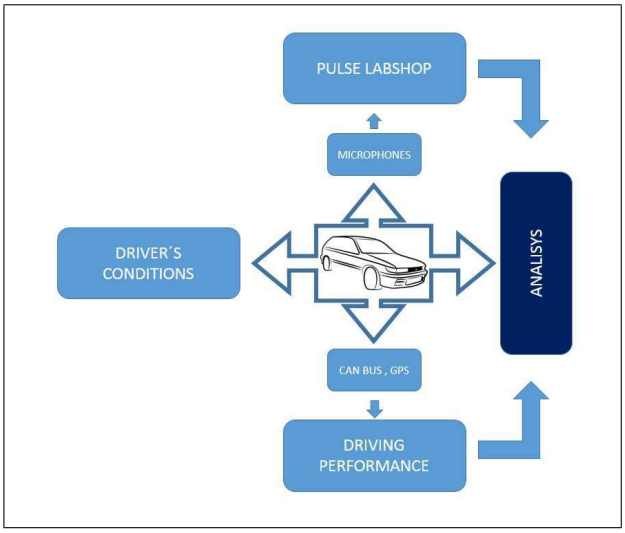

Figure 3. Experimental setup and main modules.

Figure 4. Example of a characterization of the noise emitted by an individual vehicle or by a complete urban circuit.

The PULSE LabShop system showed the measures from the engine and rolling noises of the vehicles at near-field. Concurrent driving conditions and radiated noises were measured with the vehicles running in real conditions, i.e. along the current traffic in the urban course. Before the measurements, both microphones were adjusted with a B&K 4231 sound calibrator.

Besides the microphones and the CAN BUS system to acquire acoustic data, a Vbox Lite II GPS was used to record information of the driving conditions, such as the vehicle position (latitude, longitude and altitude), vehicle

Table I. Microphone specifications.

Frequency Response: 20 to 20,000 Hz
Polar Pattern: Omnidirectional
Output Impedance: EIA rated at 165 Ω
Open Circuit Sensitivity (at 1 kHz, ref. 1V/Pascal): −34.5 dBV/Pa (19 mV)
Max SPL (1 kHz at 1% THD, 1 kΩ load): 125 dB
Equivalent Output Noise (A-weighted): 34 dB
Signal to Noise Ratio (referenced at 94 dB SPL): 60 dB
Dynamic Range at 1 kΩ load: 91 dB
Power Requirements: 11 to 52 Vdc phantom, < 2.2 mA
Common Mode Rejection: >60 dB
Polarity: Positive sound pressure on diaphragm produces positive voltage on pin 2 relative to pin 3 of output XLR connector.
Environmental Conditions: Operating Temperature Range: −18° to 70°C, Storage Temperature Range: −29° to 75°C
Cable: Shielded 1.2 meter (4 ft.) cable terminated with a 4-Pin Female Mini Connector (TA4F)

speed and acceleration (both longitudinal and lateral), and traveled distance and time.

For each of the tests, the signals from each microphone were recorded through the interface of the PULSE system, and were processed to obtain the following representations:

- The time evolution of the equivalent level of 1 s ($L_{eq,1s}$) for each of the microphones and for each test run, along the urban circuit, see Figure 5.
- The overall equivalent levels, L_{eq}, along the urban circuit, of engine and rolling noises for each test run (Table II).
- The level histograms along the circuit, Figure 6, i.e. the percentage of time that the equivalent level was in each level band.

Figure 5 shows the time evolution of $L_{eq,1s}$ of the engine and rolling noises of a gasoline, manual vehicle along an urban course. As the figure shows, this circuit contains many traffic lights, and frequent gear-shifting was necessary. Approximately one third of the total time was spent in neutral gear. Figure 6 shows the histogram levels of the time evolution of the average test runs, for the engine and rolling noises of a gasoline vehicle along the urban course. The test runs show different engine speed times, depending on whether the traffic lights were red or green. These data are not included in the respective histograms. Table II summarizes the overall Leq for the engine and rolling noises, for each driver, along the urban and suburban courses.

Although we specified the most important aspects of the variables selected, instrumentation, etc., there were factors that required changes in the parameters used, such as the type of road surface (for propagation model) or changes in the driving style of the test driver.

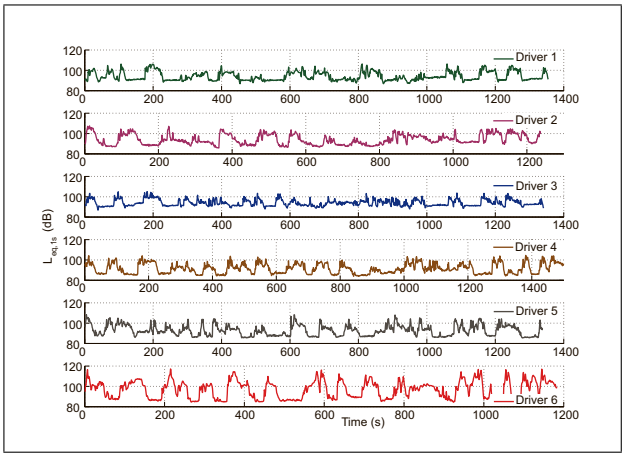

Figure 5. Time evolution of the engine noise $L_{eq,1s}$ for six runs of a gasoline vehicle along the urban course.

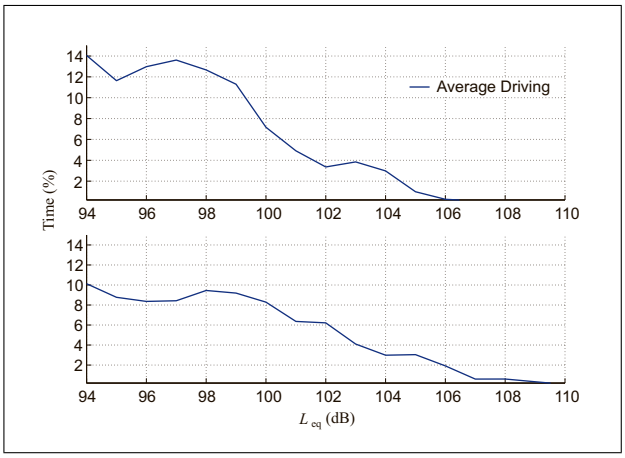

Figure 6. Histograms of the averaged runs 1-5 for engine noise (above) and rolling noise (below) $L_{eq,1s}$ along the urban course.

5. Experimental validation

Simultaneous measurements of engine, rolling, and far-field noises during pass-by tests were carried out under controlled or not controlled access; with or without traffic, with low background noise. A passenger car was driven by the same person for a set of six vehicle runs at constant speeds from 40 to 90 km/h. More specifically, the runs at 40 and 50 km/h were driven in 2nd gear, at 60 and 70 km/h the runs were driven in 3rd gear, while the 4th gear was used for runs at 80 and 90 km/h. For each pass-by, the driver maintained the vehicle speed constant over a straight part of the road about 400 m long. During the vehicle pass along the track, the noise signals picked up by the engine, rolling and extra far-field microphones were recorded using a PULSE LabShop system, which was set on a table at the side of the track. The two real field microphones moved with the vehicle. A wireless system was used to transmit the signal from each microphone to the PULSE system. Figures 7, 8 and 4 show the engine, rolling and far-field microphones, respectively, along with their corresponding transmitting packages.

Table II. Equivalent engine and rolling (tire) noise levels (dB) on urban courses, for the engine and rolling noises and for all driving.

	Gasoline vehicle							
	Suburban				Urban			
	Engine (dB)		Tire (dB)		Engine (dB)		Tire (dB)	
1	102.2		108.2		99.8		101.9	
2	105.3	$\langle L_{eq}\rangle_{1-5}$	110.4	$\langle L_{eq}\rangle_{1-5}$	100.2	$\langle L_{eq}\rangle_{1-5}$	101.2	$\langle L_{eq}\rangle_{1-5}$
3	100.3		105.7		97.8		99.7	
4	103.0	103.0	108.8	108.5	98.3	99.2	98.2	100.3
5	103.0		108.2		99.7		99.8	

Figure 7. Position of the microphone inside the engine hood, close to the air intake system (left), and position of the body pack transmitter (right).

Figure 8. Position of the microphone near the rear tire opposite to the exhaust pipe (left), and position of the body pack transmitter (right).

All the microphones were protected with a small wind screen to reduce contamination by wind-induced noise. The sensitivities of the three microphones were previously calibrated as described in section 4.

The meteorological conditions during the measurements were also included in the analysis, e.g. overcast sky, temperature of 12.6 °C, relative humidity of 58%, atmospheric pressure of 924 mb, and wind speed varying between 3 to 5 m/s.

5.1. Experimental results

The levels recorded by the three microphones are shown in Figure 9 as a function of $x = \log(V/V_{ref})$, where the vehicle speed V is expressed in km/h and the reference speed V_{ref} is set to 90 km/h. As expected, L_{tire} increases with the logarithm of the vehicle speed [32]. Engine noise decreases with vehicle speed, with a negative slope. Correspondingly, far-field noise also increases with $\log(V/V_{ref})$. The curves obtained by linear regression from the six experimental measurements are superimposed.

Figure 10 shows the 1/3 octave spectral levels of the rolling, engine and far-field noises during the pass-by experiments at 40–60 km/h, measured at each microphone.

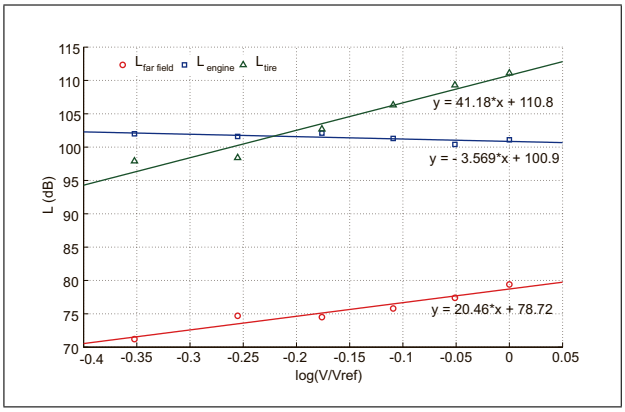

Figure 9. Noise levels for the engine, rolling and far field microphones as a function of log (V/V_{ref}) with $V_{ref} = 90$ km/h.

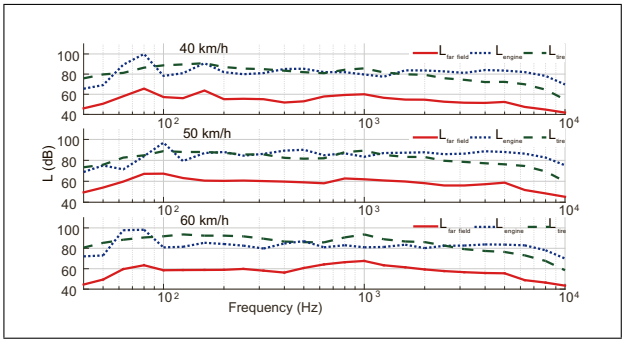

Figure 10. 1/3 octave spectral levels of the engine, rolling and far field noises radiated by the vehicle during the pass-by tests at constant speeds of 40 to 60 km/h.

As can be seen, the engine noise levels are of the same order, or even less, than the rolling noise levels.

From Figure 10, we can appreciate:

- The noise spectrum in the far-field follows very closely the pattern of the engine noise spectrum at low frequencies (below 500 Hz), while at mid-high frequencies (above 500 Hz) it follows the pattern of the rolling noise spectrum.
- The rolling noise peak at about 1000 Hz, is reproduced in the far field noise spectrum [10].
- While the rolling noise spectrum falls almost with a linear slope above 1 kHz, the engine noise spectrum remains more or less constant, and begins to decay above

4–5 kHz, possibly as a result of the effect of low-pass filter of the nose cone used by Ibarra *et al.* [3].

Table III summarizes the overall noise levels of the near- and the far-field microphones. It can be seen that, for every 10 km/h of speed increase, the engine noise varies only by 1–2 dB, the rolling noise is increased by 1-4 dB and the far-field noise increases by 1–3 dB. In other words, reducing the speed by about 10 km/h, the far field noise will decrease, on average, by 1 to 3 dB [32].

Table III. Overall noise levels (in dB) of near-field and far-field of a gasoline vehicle, for speeds of 40–90 km/h.

Speed	Gear	L_{engine}	L_{tire}	L_{farfield}
40	2	87.9	84.0	57.2
50	2	87.6	84.4	60.6
60	3	88.2	88.7	60.6
70	3	87.3	92.3	61.7
80	4	86.4	95.2	63.4
90	4	87.1	97.2	65.5

6. Model validation

The experimental far-field levels recorded by the microphone situated at 7.5 m from the center of the vehicle were compared with the far-field levels extrapolated from the engine and rolling microphones using the model developed by Ibarra et al [4, 5]. Let m1, m2 and m3 be the engine, tire and far field microphones, respectively, Figure 11. The engine microphone is located inside the engine hood, close to the air intake system, as shown in Figure 1. The tire microphone is glued below the car chassis, close to the tire, as seen in Figure 2. The far filed microphone is 7.5 m from the middle line of the vehicle and 1.2 m above the ground.

Let $P_{m1}(\omega)$, $P_{m2}(\omega)$ and $P_{m3}(\omega)$ be the sound pressure spectra at microphones m_1, m_2 and m_3, respectively. We are assuming that no other noise sources, apart from engine and rolling, are measured in the far field microphone.

$$P_{m3}(\omega) = H_1(\omega)\, P_{m1}(\omega) + H_2(\omega)\, P_{m2}(\omega), \qquad (1)$$

where $H_1(\omega)$ and $H_2(\omega)$ are the extrapolation filters between the engine and rolling and the far field microphones, respectively, Figure 11. $H_1(\omega)$ includes

$$H_1(\omega) = H_{1,\text{hood}}(\omega)\, H_{1,\text{spread}}(\omega) \cdot H_{1,\text{abs}}(\omega)\, H_{1,\text{ground}}(\omega), \qquad (2)$$

where $H_{1,\text{hood}}(\omega)$ stands for the propagation through the engine hood, $H_{1,\text{spread}}(\omega)$ includes the geometrical spreading, $H_{1,\text{abs}}(\omega)$ takes into account the sound absorption in the air, and $H_{1,\text{ground}}(\omega)$ contains the effect of ground interaction. In a similar way, $H_2(\omega)$ consists of

$$H_2(\omega) = H_{2,\text{spread}}(\omega)\, H_{2,\text{abs}}(\omega)\, H_{2,\text{ground}}(\omega). \qquad (3)$$

To account for the ground effect in the extrapolation model, a laterally discontinuous ground was considered, Figure 4 (left). We followed the recommendations of the Standard ANSI S1.18 [33] to estimate the flow resistivity of an impedance model for each of the ground types. A point source which fulfils the directional requirements of the ANSI S1.18 Standard was designed [34]. The sound pressure field generated by this source, situated at a height of 0.5 m above the ground, was picked up by two identical microphones situated at heights of 0.88 and 0.08 m respectively. The horizontal separation distance between source and microphones was fixed at 3 m. The loudspeaker was

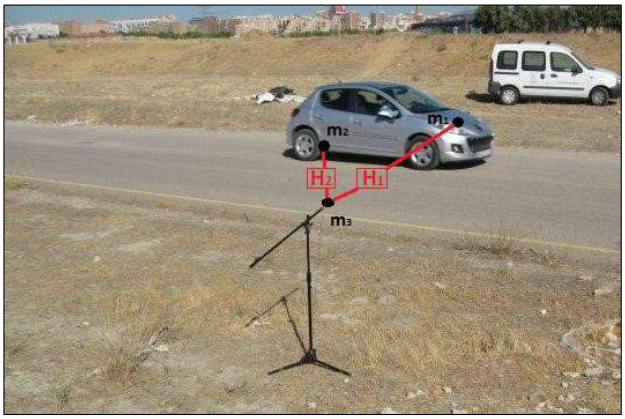

Figure 11. Measurements of noise in the near and far fields of a vehicle.

driven by a pseudo-random signal generated by a home-made virtual instrument. The instrument was created using Matlab for the determination of the impulse response functions between input and measured signals. To avoid the influence of undesired reflection and background noises, the impulse response signals were windowed and converted to the frequency domain. The meteorological conditions during the tests were recorded and included in the analyses, e.g. on one day the temperature was 12 °C, the relative humidity had a value of 48%, the atmospheric pressure was 924 mb and the wind speed was between 1.2 m/s and 3 m/s.

For determining the surface flow resistivity we calculated the level difference between top and bottom microphones for each frequency,

$$\Delta L_{\text{exp}} = 20 \log \left| \frac{p_{\text{top}}(\omega)}{p_{\text{bottom}}(\omega)} \right|. \qquad (4)$$

A predicted level difference spectrum, ΔL_{pre} can be calculated, assuming a surface as described by Miki and Hamet impedance models [35, 36]. An optimization procedure was then applied to calculate the flow resistivity that minimizes the square error between the predicted and the experimental level differences. Using this procedure, we characterized the porous asphalt of the road as having a flow resistivity of $\sigma = 7000\,\text{kP s/m}^2$, while a grass area at the side was characterized with a flow resistivity of $\sigma = 400\,\text{kP s/m}^2$. The interaction of sound with this discontinuous surface has been accounted for by using the Rasmussen model [37, 38].

Table IV. Experimental measured levels (in dB) in the far-field positions compared with the extrapolated far-field levels from the engine and rolling microphones. M1: Measured far field (0.04–10 kHz) Means/SD, E1: Extrapolated far field (0.04–10 kHz), M2: Measured far filed (0.5–10 kHz) Means/SD, E2: Extrapolated far field (0.5–10 kHz).

Speed	M1	E1	ΔL/MSE	M2	E2	ΔL/MSE
40	57.2 / 3.4	56.6	0.6 / 4.1	55.0 / 3.1	54.6	0.4 / 3.2
50	60.6 / 3.7	57.3	3.3 / 6.3	58.5 / 3.5	58.0	0.5 / 3.4
60	60.6 / 4.0	61.2	0.6 / 4.4	61.6 / 3.9	61.2	0.4 / 3.1
70	61.7 / 5.3	64.0	2.3 / 5.2	63.4 / 4.2	63.5	0.1 / 2.2
80	63.4 / 6.4	66.6	3.2 / 6.4	65.3 / 4.8	65.6	0.3 / 2.5
90	65.5 / 7.6	68.5	3.0 / 5.9	67.1 / 5.2	67.8	0.7 / 3.6

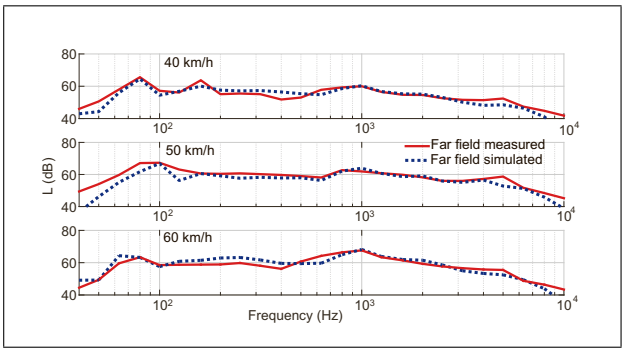

Figure 12. (colour online) Spectral noise levels measured by the far field microphone (red) and extrapolated from the near field microphones (blue), for speeds of 40–60 km/h.

The measured spectral levels at the far-field microphone were compared with the extrapolated spectral levels in Figure 12. A good agreement was obtained at frequencies above 500 Hz. Below this frequency, however, the extrapolated curves separate from the measured ones, and the separation increased as the speed of the vehicle increased. This disagreement was attributed to the wind-induced microphone noise, which was contaminating the rolling microphone below 500 Hz.

Table IV compares the measured and extrapolated overall levels at the far-field microphone, using the spectral levels at the 40 Hz-10 kHz and the 500 Hz-10 kHz frequency bands. The agreement between measured and extrapolated levels was rather good at the medium and high frequency band (500 Hz-10 kHz), with differences of less than 0.7 dB. However, the agreement degrades when the low frequencies are included and the mean squared error (MSE) increases.

As commented above, these differences are due to wind-induced microphone noise which is contaminating the rolling microphone signal. Several authors [39, 40] have reported similar problems when the rolling microphone is exposed to an air flow. They have presented several results relating the noise levels due to aerodynamic effects as a function of the vehicle speed, testing several microphone windshields.

As explained before, the placement of the sensor, in the plane of the tire, was selected considering the practicality for real-time operating conditions. It was taken into account, however, that the tire/road emission was not omnidirectional, as it is generally assumed in noise calculations. The directivity patterns had the highest values at the front of the tire [41], where the rolling noise microphone was situated, registering a horn effect.

7. Conclusions

Notwithstanding the problem with the wind-induced microphone noise below 500 Hz, the agreement between the two curves was reasonably good. The agreement between experimental and predicted levels was satisfactory, with differences of less than 0.7 dB for all the speeds tested. We conclude that, despite its simplicity, the developed semi-analytical formulation provides a correct estimation of the far-field extrapolated levels in the frequency range of 0.5–10 kHz. This could then be compared confidently with the current international regulations for road noise emissions in order to take control actions on the individual vehicles, if required.

As a result of the increasing number of vehicles on the roads in most countries, the level of road traffic noise has increased severely, despite the regulations imposed by governments and insignificant reductions in noise levels. The design of quieter vehicles, along with good design of new roads, contributes toward reducing traffic noise levels, but the reduction of those traffic noise levels has to be quantified, which is the reason that we have proposed a complete methodology to carry out noise analysis for automotive vehicles. Both, the proposed on-board system and the near- and far-fields propagation models have been validated experimentally. We expect that:

- It will enable real-time measurements of rolling and engine noises, so that the online assessment of the effectiveness to control any such noises will be easier.
- The proposed methodology allows maintaining a historical record of the noise produced by a vehicle, similar to the tachograph installed in buses and trucks. The relationship between the type of vehicle and radiated noise emitted would then be easily assessed.
- The system would facilitate the control of the individual noise emission of each vehicle during an approval test or a Technical Inspection of Vehicles.
- The proposed near-field to far-field propagation model would facilitate the integration of near-field measurements on existing noise mapping codes.

Acknowledgement

This work has been possible thanks to funding by CONACYT and ITESM.

References

[1] R. Rylander: Noise, stress and annoyance. Noise and Vibration Worldwide **3** (2006) 9–13.

[2] D. Ibarra, P. Cobo, T. Bravo: Measurement of the contribution of each individual vehicle to the road traffic noise. J. Acoust. Soc. Am. **128** (2010) 2420.

[3] D. Ibarra, P. Cobo, J. A. Calvo, J. L. San Román: Relating the near field noise of passenger cars with the driving behavior. Noise Control Eng. J. **60** (2012) 171–183.

[4] T. Bravo, D. Ibarra, P. Cobo: Far-field extrapolation of maximum noise levels produced by individual vehicles. Appl. Acoust. **74** (2013) 1463–1472.

[5] D. Ibarra, P. Cobo, F. Anfosso-Lédée: Relationship between the noise radiated by a vehicle to the near and far fields. Noise Cont. Eng. J. **61** (2013).

[6] U. Sandberg: Noise emissions of road vehicles. Effect of regulations. Final report 01-1, I-INCE, 2001.

[7] J. W. Tyler: Sources of vehicle noise. – In: Transportation Noise Reference Book. P. M. Nelson (ed.). Butterworths, London, 1987.

[8] S. Gang: Vehicle noise vibration, and sound quality. Published by SAE International. ISBN of 978-0-7680-3484-4, 2012.

[9] U. Sandberg: Tyre/road noise myths and realities. Plenary Paper, Proceedings of The International Congress and Exhibition on Noise Control Engineering, The Hague, The Netherlands, 2001.

[10] U. Sandberg: The multi-coincidence peak around 1000 Hz in tyre/road noise spectra. Proc. Euronoise, 2003, paper ID:498.

[11] J. Affenzeller, A. Rust: Road traffic noise - a topic for today and the future. VDA Technical Congress, Ingolstadt, Germany, 2005.

[12] ISO 362:1998: Acoustics – Measurement of noise emitted by accelerating road vehicles – Engineering method. International Standard Organization, Geneva, 1998.

[13] ISO 11819-1: Acoustics – Measurement of the influence of road surfaces on traffic noise – Part 1: Statistical pass-by method. International Standard Organization, Geneva, 1997.

[14] ISO/DIS 11819-2: Acoustics: Measurement of the influence of road surfaces on road traffic noise – Part 2: The close-proximity method. International Standard Organization, Geneva, 2000.

[15] ISO/PAS 11819-4: Acoustics: Method for measuring the influence of road surfaces on traffic noise – Part 4: SPB method using backing board. International Standard Organization, Geneva, 2013.

[16] M. Haider, U. Sandberg: Noise classification methods for urban road surfaces. Measurement methods. F.D12, Project SILENCE, 2006.

[17] G. J. Van Blokland, M. S. Roovers: Measurements methods. Technical Report, SILVIA Project, 2005.

[18] M. S. Roovers, H. M. Peeters: CPX-SPB/CPB relation. Technical Report, SILVIA Project, 2004.

[19] F. Anfosso-Lédée: The propagation filter between CPC and CPB measurements. SILVIA-LCPC-006-01-WP2-300404, Project SILVIA, 2004.

[20] M. Haider, G. Decornet: Noise classification methods for urban road surfaces. Classification methodology. F.D13, Project SILENCE, 2006.

[21] D. S. Cho, S. Mun: Development of a highway traffic noise prediction model that considers various road surface types. Appl. Acoust. **69** (2008) 1120–1128.

[22] D. S. Cho, S. Mun: Determination of the sound power levels emitted by various vehicles using a novel testing method. Appl. Acoust. **69** (2008) 185–195.

[23] W. Stücklschwaiger: Experimental pass-by noise source analysis. Technical report D.D10, Poject Silence, European Commission, 2006.

[24] M. Harrison: Vehicle refinement - Controlling noise and vibration in road vehicles. Elsevier Butterworth-Heinemann, Oxford, 2004.

[25] M. E. Braun, et al.: Noise source characteristics in the ISO 362 vehicle pass-by noise test: literature review. Applied Acoustics **74** (2013) 1241–1265.

[26] K. Schaaf, D. Ronneberger: Noise radiation from rolling tires-sound amplification by the horn effect. Proc. Internoise, San Francisco, USA, 1982, 131–134.

[27] K. Iwao, I. Yanazajum: A study on the mechanism of tire/road noise. JSAE Review **17** (1994) 139–144.

[28] R. A. Graf, C. Y. Kuo, A. P. Dowling, W. R. Graham: On the horn effect of a tire/road interface. Part i: Experiment and computation. J. Sound Vib. **256** (2002) 417–431.

[29] C. Miyajima, Y. Nishiwaki, K. Ozawa, T. Wakita, K. Itou, K. Takeda, F. Itakura: Driver modelling based on driving behaviour and its evaluation in driver identification. Proc IEEE **95** (2007) 427–437.

[30] J. Ko, R. Guensler, M. Hunter: Analysis of effects of driver/vehicle characteristics on acceleration noise using GPs- equipped vehicles. Transportation Research Part F **13** (2010) 21–31.

[31] A. Peterson, E. Gross: Handbook of noise measurement. General Radio Company, Concord, MA, 1963.

[32] U. Sandberg, J. A. Ejsmont: Tyre/road noise. reference book. Informex, Kisa, Sweden, 2002.

[33] ANSI S1.18: Template method for ground impedance. American National Standards Institute, Acoustical Society of America, 1999.

[34] P. Cobo, S. Ortiz, D. Ibarra, C. de la Colina: Point source equalised by inverse filtering for measuring ground impedance. Appl. Acoust. **74** (2013) 561–565.

[35] Y. Miki: Acousticals properties of porous materials – Generalizations of empirical models. J. Acoust. Soc. Jpn. (E) **11** (1990) 1.

[36] K. Attenborough, I. Bashir, S. Therzadeh: Outdoor ground impedance models. J. Acoust. Soc. Am. **129** (2011) 2806–2819.

[37] K. B. Rasmussen: Propagation of road traffic noise over level terrain. J. Sound Vib. **82** (1982) 51–61.

[38] K. B. Rasmussen: A note on the calculation of sound propagation over impedance jumps and screens. J. Sound Vib. **84** (1982) 598–602.

[39] Y. Pichaud, F. Anfosso-Lédée: Caractérisation du bruit aérodynamique du scéniclcpc nantes. Rapport des mesures réalisées en soufflerie automobile anechoique. Laboratorire Central des Ponts et Chaussées, Nantes, France, 2009.

[40] F. Anfosso-Lédée: The development of a new tire-road noise measurement device in France. Procs. 5th Symposium on Pavement Surface Characteristics, Toronto, Canada, 2004.

[41] P. Mioduszewski, J. Ejsmont: Directivity of tire/road noise emission of selected tires and pavements. Noise Control Eng. J. **57** (2009) 129–138.